Numerical and Monte Carlo Bethe ansatz method: 1D Heisenberg model

Shi-Jian Gu*

Department of Physics and Institute of Theoretical Physics,
The Chinese University of Hong Kong, Hong Kong, China

N. M. R. Peres

Departamento de Física e Centro de Física da Universidade do Minho, Campus Gualtar, P-4700-320 Braga, Portugal.

You-Quan Li

Zhejiang Institute of Modern Physics, Zhejiang University, Hangzhou 310027, P.R.China

(Dated: March 24, 2006)

In this paper we present two new numerical methods for studying thermodynamic quantities of integrable models. As an example of the effectiveness of these two approaches, results from numerical solutions of all sets of Bethe ansatz equations, for small Heisenberg chains, and Monte Carlo simulations in quasi-momentum space, for a relatively larger chains, are presented. Our results agree with those obtained by the thermodynamic Bethe ansatz (TBA). As an application of these ideas, the pairwise entanglement between two nearest neighbors at finite temperatures is studied.

PACS numbers: 75.10.Jm, 75.40.-s

I. INTRODUCTION

The study of exactly solvable models is a very important field in condensed matter physics, which began with Bethe's solution of the isotropic Heisenberg chain [1]. In general, the Bethe ansatz (BA) solution of a model has several drawbacks: it has a complex mathematical structure; the excitations are not immediately available; and most important, it does not give explicit results even for the thermodynamic quantities of the system. It was only when Yang and Yang [2] presented a strategy to study the thermodynamics of BA solvable systems that the temperature dependence of quantities such as the specific heat and the magnetic susceptibility became available. The method is now designated as the thermodynamic Bethe ansatz and has undergone many developments in the last thirty years [3]. Additionally, correlation functions, such as the conductivity, can not be obtained from the BA equations alone, and a combination of BA results with other methods is required for their calculation [4].

The BA method has been applied to Bose, Fermi[5, 6, 8], and spin systems [1, 7]. It is a general feature of the BA solution, first proved by Yang and Yang[2] for the Bose case, that a given eigenstate of the model is characterized by a unique set of quantum numbers $\{I_j\}$. Further, it also can be shown that all configurations of these quantum numbers I_j exhaust the Hilbert space of a given model. Since the energy eigenvalues are functions of the above quantum numbers, instead of using TBA and quantum Monte Carlo approaches, we can study BA solvable models in quantum number space by classical Monte Carlo method. Furthermore, for a small system (these systems are larger than those which exact diagonalization methods can be applied), it is possible to solve the BA equations for all eigenvalues. Therefore, the expectation value of an Hermitian operator in thermal equilibrium can be computed.

In this paper, we shall introduce two numerical approaches for computing thermodynamic quantities of Bethe ansatz solvable models. The methods are illustrated with the 1D isotropic Heisenberg model, since this model is well studied in the literature. Furthermore, the study of the Heisenberg model is itself relevant, since this system predicts many properties of quasi-one-dimensional materials [10–12]. This model has been investigated by many kinds of methods. For example, the low temperature behaviors are quite well understood by a combination of the Bethe ansatz [13] and conformal field theory [14, 15]. A strong logarithm singularity in the susceptibility at low temperature was first found by the Bethe ansatz calculation of the quantum transfer matrix (QTM) [16] and then verified experimentally [10, 11]. The thermodynamics of the model has been studied by TBA [3, 17–22] as well as by QTM [23–26]. As an application of our method, we apply it to the pairwise entanglement of two nearest neighbors of this model at finite temperatures. The entanglement in spin systems has attracted much attention[27–29] due to its nontrivial role in the field of quantum information and quantum computation[30, 31], moreover, it also sheds new light on our understanding of the quantum critical phenomenon [32, 33].

The paper is organized as follows. In Sec. II, we first briefly review the BA solution of the isotropic Heisenberg model. In Sec. III and Sec. IV, we introduce the basic idea of the numerical Bethe ansatz (NBA) and Monte Carlo Bethe ansatz (MCBA). In Sec.V, we check the effectiveness of these two methods by computing the specific heat and the magnetic susceptibility in the ab-

*Email: sjgu@phy.cuhk.edu.hk
URL: http://www.phystar.net/

sence of an external magnetic field and compare our results with those obtained from the TBA. We then use our methods to study the two quantities above in the presence of an external magnetic field. In Sec. VI, we apply our method to study the behavior of the pairwise entanglement in the antiferromagnetic Heisenberg model. Finally, a brief summary is given in Sec. VII.

II. ISOTROPIC HEISENBERG MODEL

Now let us first review the Bethe ansatz solution of the 1D Heisenberg chain, which can be found in Takahashi's book [3]. The Hamiltonian of the isotropic Heisenberg model is

$$\mathcal{H} = -J\sum_{l=1}^{N}\left(S_l^x S_{l+1}^x + S_l^y S_{l+1}^y + S_l^z S_{l+1}^z\right), \qquad (1)$$

where N is the number of sites, S_l^x, S_l^y, S_l^z are spin $1/2$ operators at site l and $J = -1, 1$ representing anti-ferromagnetic and ferromagnetic cases, respectively. The solution with a periodic boundary condition $\vec{S}_{N+1} = \vec{S}_1$ using the string hypothesis takes the form

$$N\theta(x_\gamma^n/n) = 2\pi I_\gamma^{(n)} + \sum_{m,\beta\neq n,\gamma} \Theta_{nm}(x_\gamma^n - x_\beta^m). \qquad (2)$$

Here $\theta(x) = 2\tan^{-1}(x)$, and

$$\begin{aligned}
\Theta_{nm}(x) &= \theta\left(\frac{x}{|n-m|}\right) + 2\theta\left(\frac{x}{|n-m|+2}\right) + \cdots + 2\theta\left(\frac{x}{n+m-2}\right) + \theta\left(\frac{x}{n+m}\right) \quad \text{For} : n \neq m \\
&= 2\theta\left(\frac{x}{2}\right) + 2\theta\left(\frac{x}{4}\right) + \cdots + 2\theta\left(\frac{x}{2n-2}\right) + \theta\left(\frac{x}{2n}\right) \quad \text{For} : n = m
\end{aligned} \qquad (3)$$

and x_γ^n is the real part of the n-string which is designated by

$$x_\gamma^{n,j} = x_\gamma^n + i(n+1-2j), \quad j = 1,\ldots,n$$

I_γ^n is the quantum number of γth n-string (note that n and γ are indices). We denote the number of the n-string by α_n, thus $n = 1,\ldots,M$; $\gamma = 1,\ldots,\alpha_n$ and the string configuration $\{\alpha\}$ satisfy

$$\alpha_1 + 2\alpha_2 + \cdots + (M-1)\alpha_{M-1} + M\alpha_M = M, \qquad (4)$$

where M is the number of down spins. The quantum number of n-string I_γ^n is an integer (half-odd integer) if $N - \alpha_n$ is odd (even) and satisfy

$$|I_\alpha^n| \leq \left(N - 1 - \sum_{m=1}^{M} t_{nm}\alpha_m\right)/2, \qquad (5)$$

where $t_{nm} \equiv 2\min(n,m) - \delta_{nm}$. For a given set of $\{I_\gamma^n\}$, Eq. (2) can be solved numerically and the energy is given by

$$E\{I_\gamma^n\} = -NJ/4 + \sum_{n,\gamma} \frac{2Jn}{(x_\gamma^n)^2 + n^2}, \qquad (6)$$

which represents the energy of the lowest weight state in the SU(2) irreducible space designated by $S = N/2 - M, S_z = S, S-1,\ldots,-S$. In the presence of an external field h a Zeeman term is added to Eq. (6). Hence the total energy of a given quantum number configuration is given by

$$E = E\{I_\gamma^{(n)}\} - h\mathcal{M}, \qquad (7)$$

where $\mathcal{M} = 2S_z$ is the magnetization of the state.

III. NUMERICAL BETHE ANSATZ

In statistical mechanics, the expectation value of a Hermitian operator Q in thermal equilibrium is given by

$$\langle Q \rangle = \frac{1}{Z}\sum_\mu Q_\mu e^{-\beta E_\mu}. \qquad (8)$$

where Z is known as the partition function, defined as

$$Z = \sum_\mu e^{-\beta E_\mu}, \qquad (9)$$

β is inverse temperature, and $\sum_\mu$ represents the sum over all possible eigenstates of the Hamiltonian. It turns out that the variation of Z with respect to temperature or any other external parameters affecting the system can tell us virtually everything we might want to know about the macroscopic behavior of the system. For example, the internal energy is given by

$$U = \frac{1}{Z}\sum_\mu E_\mu e^{-\beta E_\mu} \qquad (10)$$

From Eq. (9), it is easy to see that the internal energy can also be written in terms of a derivative of the partition function:

$$U = -\frac{1}{Z}\frac{\partial Z}{\partial \beta} = -\frac{\partial \ln Z}{\partial \beta}. \tag{11}$$

The specific heat is given by the derivative of the internal energy:

$$C_v = \frac{\partial U}{\partial T} = -k_B\beta^2\frac{\partial U}{\partial \beta} = -k_B\beta^2\frac{\partial^2 \ln Z}{\partial \beta^2}. \tag{12}$$

where k_B is the Boltzmann constant which is set to unity hereafter.

Our aim is to combine the idea of statistical mechanics mentioned above with the numerical solution of the BA equations. The main idea of the numerical Bethe ansatz method we introduce here is, first, to compute all eigenvalues of a BA solvable model from its corresponding BA equations. Then to compute the expectation value of the Hermitian operators, representing the physical observables we are interested in, by averaging those operators over all states of the system, weighting each state with its own Boltzmann weight.

It has been shown [3] that the Hilbert space of the isotropic Heisenberg model is complete under the string classification. Here we want to show how to travel through all $C_{N/2}^N$ states in quantum number space and illustrate it by considering a system of 6 sites.

For the case of M down spins, the first task is how to obtain all string configurations fulfilling the restriction (4). We adopt a time-like number "$\alpha_M : \alpha_{M-1} : \cdots : \alpha_2 : \alpha_1$", where the magnitude α_n measures from 0 to $[M/n]$ (here $[x]$ returns the truncated integer value of x), just like hours and minutes in "HH:MM" measure from 0 to 23 and 0 to 59 respectively. If we increase the number "$\alpha_M : \cdots : \alpha_1$" by adding 1 to the first digit α_1, step by step, we can travel through all possible values. Among all these numerical values, only those whose digits satisfy the condition (4) are what we need. Then all string configurations can be found by this procedure. Of course, these operations are realized in a computer. In order to make the method clear, let us consider a problem of 6 sites.

M=0: It is easy to have the state with all spins up, i. e. $M = 0$, which has energy $E = -JN/4$.

M=1: In this case, we only have one string configuration $\alpha_1 = 1$ and one quantum number $-2 \leq I_1 \leq 2$, thus there are 5 states. Each of them is represented by one quantum number in the interval $[-2, 2]$. We can get all possible quantum number configurations from the following figure,

$$- - \circ - - \circ - - \bullet - - \circ - - \circ - -$$

where the dot is the occupied quantum number, and the open circles represent other possible quantum numbers. Then the BA equation is just

$$6\tan^{-1}x_1^1 = \pi I_1, \tag{13}$$

TABLE I: All quantum number configurations for $M = 2$.

$\alpha_1 = 2, \alpha_2 = 0$	I_1^1	-1.5	-1.5	-1.5	-0.5	-0.5	0.5
	I_2^1	-0.5	0.5	1.5	0.5	1.5	1.5
$\alpha_1 = 0, \alpha_2 = 1$	I_1^2	-1	0	1	-	-	-

which has a simple solution $x_1 = \tan(\pi I_1/6)$.

M=2: Here the string configuration is characterized by $\{\alpha_1, \alpha_2\}$. We construct a number "$\alpha_2 : \alpha_1$", in which the maximum value of α_1 is 2 ($[2/1] = 2$), and α_2 1 ($[2/2] = 1$). Increasing α_1 step by step we generate all possible configurations of the "$\alpha_2 : \alpha_1$" number, ranging from 0:0 to 1:2. Among all the generated configurations, we are only interested in those satisfying the condition $\alpha_1 + 2\alpha_2 = 2$. The first case is $\alpha_1 = 2, \alpha_2 = 0$, in which the quantum numbers satisfy $-1.5 \leq I_1^1, I_2^1 \leq 1.5$, the second one is $\alpha_1 = 0, \alpha_2 = 1$, in which the number satisfies $-1 \leq I_1^2 \leq 1$. They can be characterized by

$$- - \circ - - \bullet - - \bullet - - \circ - -$$

and

$$- - - \circ - - \ddagger - - \circ - - -$$

respectively, where $\ddagger$ denotes the occupation for a quantum number of 2-string. In Table I, we list all quantum number configurations for $M = 2$. The BA equations for these two cases are

$$6\tan^{-1}x_1^1 = \pi I_1^1 + \tan^{-1}\frac{x_1^1 - x_2^1}{2},$$
$$6\tan^{-1}x_2^1 = \pi I_2^1 + \tan^{-1}\frac{x_2^1 - x_1^1}{2}, \tag{14}$$

and

$$6\tan^{-1}(x_1^2/2) = \pi I_1^2, \tag{15}$$

respectively.

M=3: In this case the string configuration is characterized by $\{\alpha_1, \alpha_2, \alpha_3\}$. In the same way as we did above, we construct a number "$\alpha_3 : \alpha_2 : \alpha_1$", the maximum value for each digit from left to right is 1, 1, 3 respectively. Then we have 3 string configurations with the condition $\alpha_1 + 2\alpha_2 + 3\alpha_3 = 3$, which correspond to the following sequences

$$a: \quad - - - - \bullet - - \bullet - - \bullet - - - -$$

$$b: \quad - - - - \circ - - \bullet - - \circ - - - -$$
$$- - - - - - - \ddagger - - - - - - -$$

$$c: \quad - - - - - - \S - - - - - - -$$

$\alpha_1 = 3, \alpha_2 = 0, \alpha_3 = 0$	I_1^1	-1.0	-	-
	I_2^1	0	-	-
	I_3^1	1.0	-	-
$\alpha_1 = 0, \alpha_2 = 0, \alpha_3 = 1$	I_1^1	-1.0	0	1.0
	I_1^2	0	0	0
$\alpha_1 = 1, \alpha_2 = 1, \alpha_3 = 0$	I_1^3	0	-	-

where a, b, c have 1, 3, 1 states respectively, § denotes the site for 3-string. And in Table II, we list all quantum number configurations for $M = 3$, whose BA equations are

$$
\begin{aligned}
6\tan^{-1} x_1^1 &= \pi I_1^1 + \tan^{-1}(x_1^1 - x_2^1) \\
&\quad + \tan^{-1}(x_1^1 - x_3^1), \\
6\tan^{-1} x_2^1 &= \pi I_2^1 + \tan^{-1}(x_2^1 - x_1^1) \\
&\quad + \tan^{-1}(x_2^1 - x_3^1), \\
6\tan^{-1} x_3^1 &= \pi I_3^1 + \tan^{-1}(x_3^1 - x_1^1) \\
&\quad + \tan^{-1}(x_3^1 - x_1^1).
\end{aligned} \tag{16}
$$

$$
\begin{aligned}
6\tan^{-1} x_1^1 &= \pi I_1^1 + \tan^{-1}(x_1^1 - x_1^2) \\
&\quad + \tan^{-1}((x_1^1 - x_1^2)/3), \\
6\tan^{-1} x_1^2 &= \pi I_1^2 + \tan^{-1}(x_1^2 - x_1^1) \\
&\quad + \tan^{-1}((x_1^2 - x_1^1)/3),
\end{aligned} \tag{17}
$$

and

$$
6\tan^{-1} x_1^3 = \pi I_1^3. \tag{18}
$$

respectively.

As a result we have in total $C_3^6 = 20$ distinct configurations of a quantum number whose Hilbert space is complete.

Then, we compute the eigenvalue for a given quantum number configuration $\{I_\gamma^n\}$ by solving the BA equations numericaly. For the Heisenberg chain, the BA equations can be solved by iteration, for other models, such as the Hubbard model, the BA equations can be solved by a gradient method.

IV. MONTE CARLO BETHE ANSATZ

For a system of N sites, there are $C_{N/2}^N$ quantum number configurations. This number increases exponentially with the size of the system, so it is impossible to calculate all eigenvalues for a large system, such as $N > 40$, with existing computer capacity. This restriction can be overcome by a Monte Carlo method. There are many Monte Carlo methods available, and we introduce below a new method that we call the Monte Carlo Bethe ansatz. This method is a classical Monte Carlo strategy applied to a quantum problem. The basic idea behind the MCBA method is to simulate the random thermal fluctuation of the system from state to state in the quantum number space of the BA solution. This method is not limited by the sign problem that may show up in the usual quantum Monte Carlo methods.

Since the energy eigenvalues are a function of both M and of the quantum numbers I_γ^n we can follow a classical Monte Carlo strategy, by sampling the configuration space of M and $\{I_\gamma^n\}$. We now explain how to implement the Monte Carlo calculation, which follows three steps. Let us assume the present state is μ with a corresponding M_μ – the number of down spins in state μ. From the state μ any other state ν with M_ν, within the number of $C_{N/2}^N - 1$, can be obtained.

step one: first we choose M_ν, knowing that the number of states with M_ν spins down is $C_{M_\nu}^N - C_{M_\nu - 1}^N$, thus the probability of selecting M_ν is $(C_{M_\nu}^N - C_{M_\nu - 1}^N)/C_{N/2}^N$.

step two: having selected M_ν, all possible string configurations for the given M_ν are determined from of Eq. (4) which satisfy [3]

$$
\sum_{\alpha_1 + \cdots + M\alpha_M = M} D(\{\alpha_n\}) = (C_M^N - C_{M-1}^N), \tag{19}
$$

where $D(\{\alpha_n\})$ is the number of states, characterized by the set of quantum numbers $\{I_\alpha^n\}$ associated with the string configuration $\{\alpha_n\}$, and reads

$$
D(\{\alpha_n\}) = \prod_{i=1}^M C_{\alpha_j}^{N - \sum_{j=1}^M t_{ij}\alpha_j}. \tag{20}
$$

So, in step two, we select a string configuration with the probability $D(\{\alpha_n\})/(C_M^N - C_{M-1}^N)$.

step three: having determined the string configuration, we then select at random a quantum number configuration, which is the state ν we want, for the given string configuration. From the partition function Z, the probability density for a state μ is

$$
p_\mu = (N - 2M_\mu + 1)e^{-\beta E_\mu}, \tag{21}
$$

where the degenerancy of state μ was taken into account. The detailed balance condition tells us the transition probability should satisfy

$$
\frac{p_\nu}{p_\mu} = \frac{(N - 2M_\nu + 1)}{(N - 2M_\mu + 1)} e^{-\beta(E_\nu - E_\mu)}. \tag{22}
$$

Hence it is possible to use the Metropolis algorithm for the acceptance ratio to accept or reject the state μ according to

$$
A(\mu \to \nu) = \begin{cases} \frac{(N-2M_\nu+1)}{(N-2M_\mu+1)}e^{-\beta(E_\nu - E_\mu)}, & \frac{p_\nu}{p_\mu} < 1 \\ 1, & \text{otherwise.} \end{cases} \tag{23}
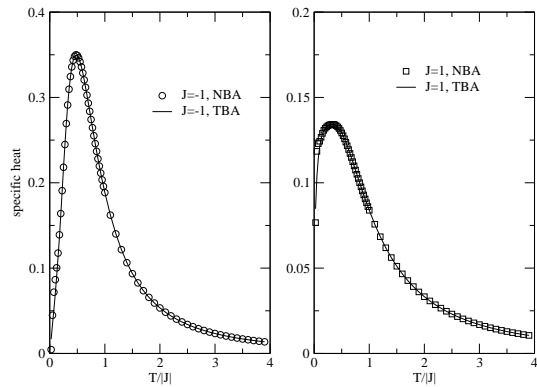$$

FIG. 1: The specific heat of a 24 site anti-ferromagnetic (left) and ferromagnetic (right) XXX model and the same quantities ob
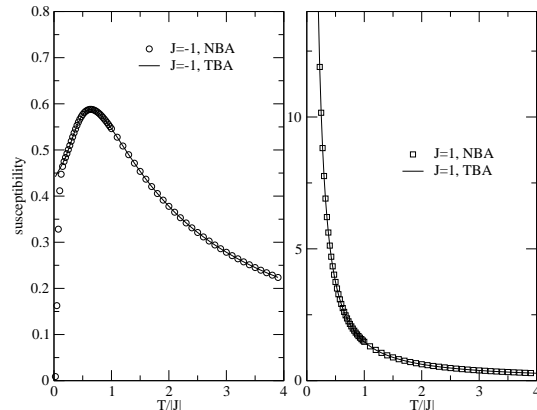

FIG. 2: The susceptibility of a 24 site anti-ferromagnetic (left) and ferromagnetic (right) XXX model (points) and the same quantities obtained by TBA (lines).

The MCBA algorithm is complete and the three basic steps are repeated a number of times. After an initial equilibration time, the expectation values can be then estimated as an arithmetic mean over the repeated Markov chain

$$\langle Q \rangle = \frac{1}{N} \sum_{\{\mu\}} Q(\mu). \tag{24}$$

V. SPECIFIC HEAT AND SUSCEPTIBILITY

In order to check the validity of our approaches, we apply these two methods to the study of the specific heat and the magnetic susceptibility of the anti-ferromagnetic and ferromagnetic Heisenberg models.

For the present model, however, because of the degeneracy in each set of quantum number configurations, Eq. (8) should be revised according to the property of the operator. For example, the internal energy and magneti-
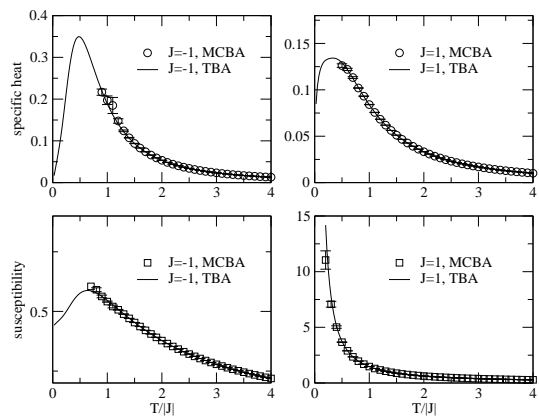

FIG. 3: The specific heat and susceptibility for a 60 site chain, computed with the MCBA method, is compared with the TBA results (**lines**) both for the anti-ferromagnetic (**circles**) and ferromagnetic (**squares**) cases.

zation are

$$\langle E \rangle = \frac{1}{Z} \sum_{\mu} (N - 2M_\mu + 1) E_\mu e^{-\beta E_\mu},$$

$$\langle M \rangle = \frac{1}{Z} \sum_{\mu} \sum_{M_\mu^z = -N/2 + M_\mu}^{N/2 - M_\mu} 2M_\mu^z e^{-\beta E_\mu}. \tag{25}$$

where $Z = \sum_{\mu} (N - 2M_\mu + 1) e^{-\beta E_\mu}$. From thermodynamics it is easy to obtain the expression for the specific heat and magnetic susceptibility per site

$$C = \frac{\beta^2}{N} (\langle E^2 \rangle - \langle E \rangle^2),$$

$$\chi = \frac{\beta}{N} (\langle M^2 \rangle - \langle M \rangle^2) \tag{26}$$

We apply NBA to a 24-site system and MCBA to a 60-site system, respectively. The latter has C_{30}^{60} different quantum number configurations, hence it is impossible to calculate all the eigenvalues of the system.

In Figs. 1 and 2, we show the specific heat and the magnetic susceptibility, for a 24-site system, obtained from NBA and compare our results with those obtained from TBA. It is clear that the two results match. In Fig 3, we show the specific heat and the magnetic susceptibility, for a 60-site system obtained from MCBA together with the results from TBA. They both agree to each other except at low temperature. In Table V, we compare, for the ferromagnetic case, the two methods we introduced here with TBA, giving the explicit numerical values. It is clear that our methods work very well for the present model. Hence our conclusion is that for a small system, such as $N \leq 38$ due to the computer limitation, it is possible to compute all eigenvalues and to obtain all possible thermodynamic quantities of interest by using Eq. (8). For temperatures larger than the finite size energy gap our results agree with TBA results exactly. For larger
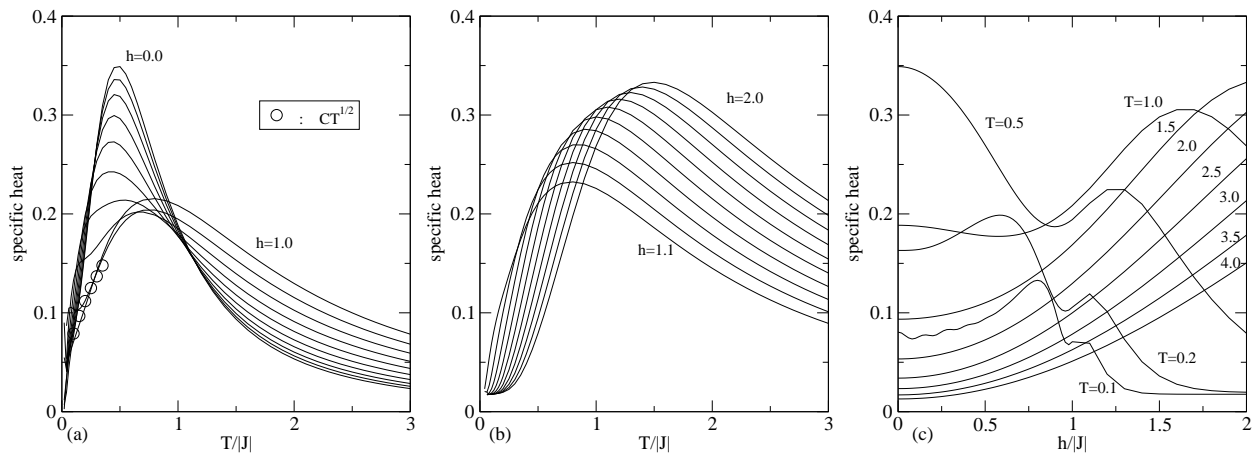
FIG. 4: The specific heat of the anti-ferromagnetic Heisenberg model for different values of the external field: (a) $h = 0, 0.2, 0.3, \ldots, 1.0$; (b) $h = 1.1, 1.2, \ldots, 2.0$; (c) specific heat as a function of h for different temperatures $T = 0.1, 0.2, \ldots, 4.0$. In panel (a) of fit to the law $C = \propto T^{1/2}$, for $h = 1.0$, is given at low temperatures.
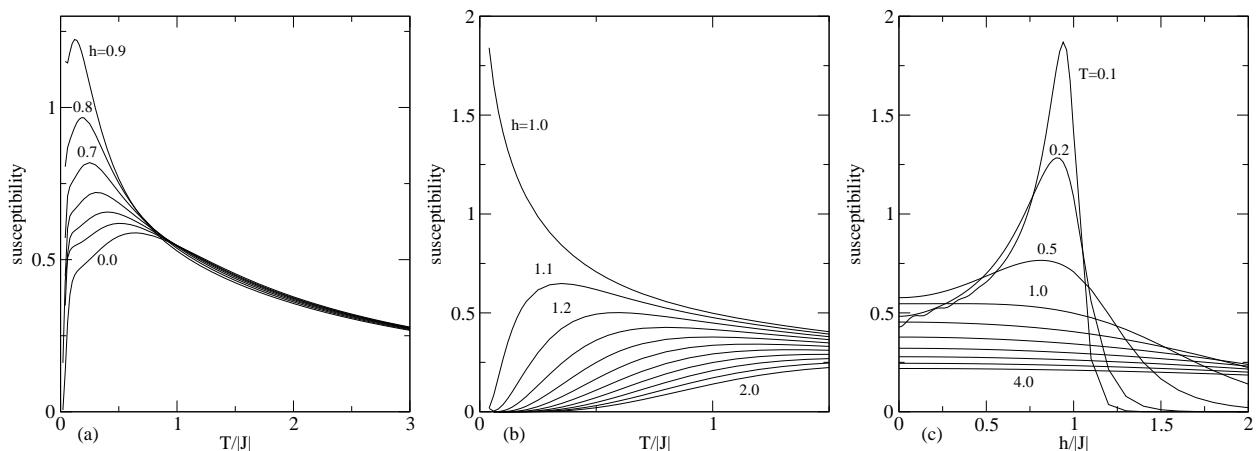

FIG. 5: The magnetic susceptibility of the anti-ferromagnetic Heisenberg model for different values of the external field: (a) $h = 0, 0.4, 0.5, \ldots, 0.9$; (b) $h = 1.0, 1.2, \ldots, 2.0$; (c) magnetic susceptibility as a function of h for different temperatures $T = 0.1, 0.2, \ldots, 4.0$.

systems, however, results can still be obtained by using the MCBA method. For the present model, it is interesting that the result of the 24-site system already matches that obtained from NBA for thermodynamic system. We interpret this being due to the fact that the correlation functions in this model are all power-law decay. Therefore, the local physical quantities, such as energy, are not effected remarkably by those spins that are far away. So a small system can well describe the thermal properties of an infinite system.

Now we study the thermodynamics of the model in the presence of a magnetic field by NBA, which has also been studied by Klümper [26]. In Fig. 4 and Fig. 5, the results for the specific heat and the magnetic susceptibility of the anti-ferromagnetic case are shown for various magnetic fields. It is clear from these two figures

that there are two different behaviors at low temperature, separated by the saturation field $h_c = 1.0$ in the ground state. In order to understand better this behavior of the antiferromagnetic case, let us use the mapping between the Heisenberg model and the spinless fermion model. This mapping is achieved by the Jordan-Wigner transformation [36], and Hamiltonian (1) can be written as

$$
\mathcal{H} = -\frac{J}{2} \sum_{l=1}^{N} (f_l^\dagger f_{l+1} + f_{l+1}^\dagger f_l)
$$

$$
+ J \sum_{l=1}^{N} (n_l - \frac{1}{2})(n_{l+1} - \frac{1}{2}). \qquad (27)
$$

where the spinless fermion operators $f_l^\dagger, f_l$ obey the usual anti-commutation relation, n_l is the usual local number
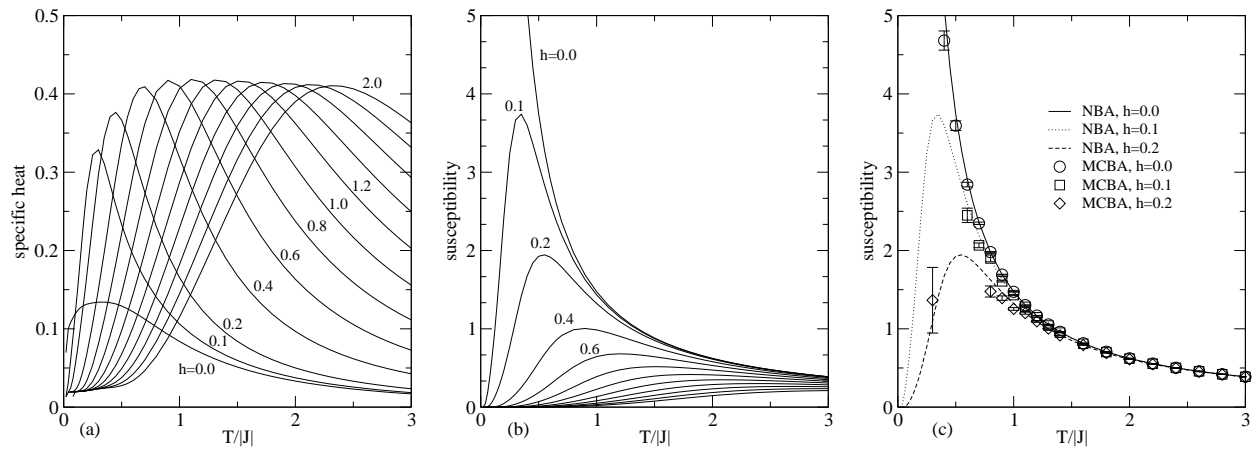
FIG. 6: The specific heat(a) and the magnetic susceptibility(b) for the ferromagnetic Heisenberg model as a function of temperature for different values of an external field $h = 0.0, 0.1, 0.2, \ldots, 2.0$, obtained by NBA. (c). The susceptibility of ferromagnetic Heisenberg model for $h = 0.0, 0.1, 0.2$, obtain by NBA and MCBA respectively.

TABLE III: Specific heat and susceptibility of ferromagnetic XXX model obtained by a thermodynamic Bethe ansatz (TBA), a numerical Bethe ansatz (NBA) solution of a 24 site system, and a Bethe ansatz based Monte Carlo (MCBA) approach for a 60 site system.

	T/J	TBA	NBA	MCBA
C_v	0.5	0.129178	0.129197	0.1261 ± 0.0019
	0.6	0.121671	0.121688	0.1220 ± 0.0012
	0.7	0.112363	0.112379	0.1132 ± 0.0009
	0.8	0.102496	0.102511	0.1019 ± 0.0003
	0.9	0.092861	0.092875	0.0931 ± 0.0002
	1.0	0.083875	0.083887	0.0840 ± 0.00017
	1.5	0.051111	0.051117	0.05112 ± 0.00004
	2.0	0.033256	0.033260	0.03326 ± 0.00002
	2.5	0.023088	0.023090	0.02308 ± 0.00001
	3.0	0.016876	0.016878	0.01687
χ	0.5	3.7378	3.742446	3.669 ± 0.027
	0.6	2.90686	2.909917	2.8914 ± 0.0139
	0.7	2.35856	2.360709	2.3458 ± 0.0039
	0.8	1.97323	1.974817	1.9613 ± 0.0044
	0.9	1.68953	1.690744	1.6902 ± 0.0028
	1.0	1.473032	1.473986	1.47509 ± 0.00180
	1.5	0.882613	0.882996	0.88316 ± 0.00016
	2.0	0.622855	0.623056	0.62299 ± 0.00010
	2.5	0.479082	0.479205	0.47908 ± 0.00007
	3.0	0.388433	0.388516	0.38848 ± 0.00004

operator. When $h < h_c$, the system is not fully polarized, that is $\sum_{l=1}^{N} n_l > 0$, hence we always have two Fermi points $\pm k_F$ in the ground state. The dispersion relation of low-lying excitations is dominated by the linear-k dependence, hence we still have the Fermi-liquid like specific heat: $C \propto T$ at low temperatures. If $h \geq h_c$, however, and from the point view of spinless fermions, we have $\sum_{l=1}^{N} n_l = 0$, and the dispersion relation becomes k^2, because of the $\cos k$ dispersion-relation for the

fermions in the lattice. Hence, the specific heat manifests a $T^{1/2}$ behavior at sufficiently low temperature for $h = h_c$, which can be seen in Fig. 4 (open circles). Moreover, the magnetic susceptibility presents a strong peak for $h = h_c$, when $T \to 0$ [see Fig. 5, panel (c)]. This strong magnetic response is associated with a change in the nature of the elementary excitations when the line $h = h_c$ is crossed at zero temperature. Indeed, at $T = 0$ and $h_c = 1.0$, the system manifests infinite susceptibility, as can be seen from Fig. 5, panel (b). We attribute it due to the degeneracy between the state of $[N-1, 1]$ and $[N]$, and a small magnetic field can fully polarize the system. The phase with $h \geq h_c$ shares anti-ferromagnetic-like behavior [Fig. 6, panel (b)], while for $h < h_c$, the susceptibility shows a logarithm singularity [26].

For the ferromagnetic case the specific heat and the magnetic susceptibility are plotted in Fig. 6, for different values of the magnetic field. As is known, if $h = 0$ the ground state of the ferromagnetic case is highly degenerate with $S = N/2, S_z = -S, -S + 1, \cdots, S$ and a very small h can fully polarize the system. So it is easy to understand why zero temperature susceptibility is infinite. After it is magnetized (in the presence of small h), however, the susceptibility should be zero. This behavior is seen in Fig. 6, panel (b). We also show, in Fig. 6, panel (c), the susceptibility obtained by MCBA. Both the results of the two methods agree with each other perfectly.

VI. PAIRWISE ENTANGLEMENT AT FINITE TEMPERATURES

As an application, we apply our method to the pairwise entanglement of two nearest neighbors at finite temperatures. Obviously, the Hamiltonian is invariant under a global SU(2) rotation, which implies total spin conservation. Thus the reduced density matrix of any two spins
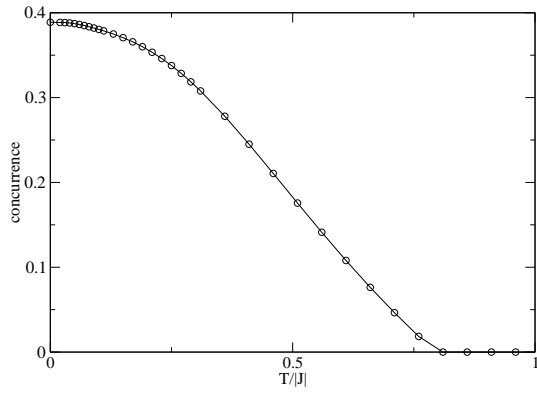
FIG. 7: The concurrence as a function of the temperature for a 30 site anti-ferromagnetic XXX model.
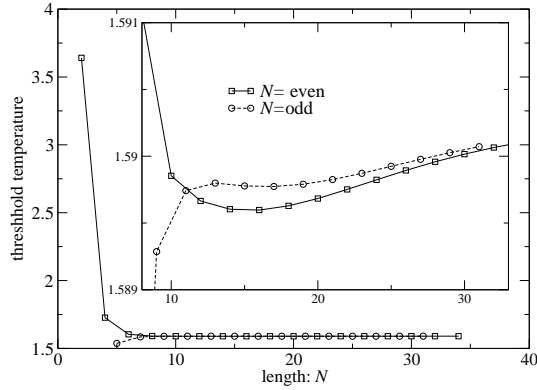

FIG. 8: The threshold temperature of concurrence of anti-ferromagnetic XXX model for different sizes of system. In order to compare with previous work[28], the threshold temperature is in units of $|J|/2$.

of the system takes the form

$$\rho_{jl} = \begin{pmatrix} u^+ & 0 & 0 & 0 \\ 0 & w_1 & z & 0 \\ 0 & z^* & w_2 & 0 \\ 0 & 0 & 0 & u^- \end{pmatrix}, \tag{28}$$

which is expressed in the conventional bases $|\uparrow\uparrow\rangle$, $|\uparrow\downarrow\rangle$, $|\downarrow\uparrow\rangle$, $|\downarrow\downarrow\rangle$. The entities of the reduced density matrix (28) can be calculated from the finite-temperature correlation functions, $G^{\alpha\beta} = \langle S^\alpha S^\beta \rangle$, namely

$$u^+ = u^- = \frac{1}{4}(1 + 4G^{zz}),$$
$$z = G^{xx} + G^{yy} + iG^{xy} - iG^{yx}. \tag{29}$$

For the present model, we also have $G^{xx} = G^{yy} = G^{zz}$ due to the global SU(2) symmetry. Since we just consider the entanglement between the nearest neighbors,

the correlation function is simply

$$G^{\alpha\alpha} = -\frac{1}{3JN}\langle E \rangle, \tag{30}$$

where $\langle E \rangle$ is calculated from Eq. (25). Then, the pairwise entanglement, in terms of the measurement of concurrence[37], can be calculated as

$$C = 2\max\left[0, |z| - \sqrt{u^+ u^-}\right] \tag{31}$$

which is site-independent because of the translational invariance.

We show the concurrence between two nearest neighbors as a function of temperature for a 30-site system in Fig. 7. From the figure we can see that the thermal fluctuation usually suppresses the entanglement. Meanwhile, in the high temperature limit, $T \to \infty$, the Boltzmann weight of each eigenstate becomes almost equal, this fact leads to vanishing correlation functions. Therefore, the concurrence is expected to become zero in the high temperature region. So there exists a threshold point T_{th} at which the concurrence becomes zero as the temperature increases. The threshold temperature is quite important since it tells us the range of temperature in which the system has nonzero entanglement. As is well known, in spin $1/2$ systems, the nearest neighbor superexchange interaction is estimated in the order of 1000K. The above result shows that the threshold temperature is also in the same order of the interaction strength. Therefore the entanglement of two nearest neighbors may always exist at room temperature. In order to study the dependence of the threshold temperature on the system's size, we show the behavior of the threshold temperature in Fig. 8 for the system-size up to 32. From the figure, we find $T_{\text{th}}(N = \text{odd}) < T_{\text{th}}(N = \text{even})$ if $N < 11$[28]. However, this relation is not longer true if $N > 11$, as we can see from the figure. It becomes $T_{\text{th}}(N = \text{odd}) > T_{\text{th}}(N = \text{even})$.

VII. SUMMARY

In summary, we presented two numerical approaches to the thermodynamics of Bethe ansatz solvable models. The first one is the numerical Bethe ansatz which works very well for a small system. We think it is possible to obtain all eigenvalues of a system up to size $L = 38$, for the Heisenberg model. For a relatively larger system, we also find that the Monte Carlo simulation in quasi-momentum space works well in the moderate and high temperature regions. At low temperatures, the present selection method is not excellent, and a better one is required. The discovery of such a method is a challenging and interesting research problem. As an application, we used NBA to study the behavior of pairwise entanglement and the corresponding threshold temperature in the antiferromagnetic Heisenberg model. We found that

the finite-size-effect of the threshold temperature shows a quite different behavior for even- and odd-size systems.

There are many physical quantities of interest at finite temperature which are still not well understood, such as spin stiffness of the XXZ model that is important to understand the transport properties, because of the complex form of the thermodynamic equations. Our methods provide a new route to compute all these quantities directly from the Bethe ansatz equations.

[1] H. A. Bethe, Z. Physik **71**, 205 (1931). H. A. Bethe, reprinted (translation) paper by Daniel C. Mattis in *The Many-Body Problem - An Encyclopedia of Exactly Solved Models in One Dimension*, (World Scientific, Singapore, 1993), page 689.

[2] C. N. Yang and C. P. Yang, J. Math. Phys. **10** 1115 (1969).

[3] M. Takahashi, *Thermodynamics of One-Dimensional Solvable Models*, (Cambridge 1999).

[4] J. M. P. Carmelo, N. M. R. Peres, and P. D. Sacramento, Phys. Rev. Lett. **84**, 4673 (2000).

[5] E. H. Lieb and W. Liniger, Phys. Rev. **130**, 1605 (1963).

[6] C. N. Yang, Phys. Rev. Lett. **19**. 1312 (1967).

[7] R. Orbach, Phys. Rev. **112**, 309 (1958).

[8] E. L. Lieb and F. Y. Wu, Phys. Rev. Lett **20**, 1445 (1968).

[9] B. Sutherland, Phys. Rev. Lett. **20**, 98 (1968).

[10] N. Motoyama, H. Eisaki, and S. Uchida, Phys. Rev. Lett. **76**, 3212 (1996).

[11] S. Takagi, H. Deguchi, K. Takeda, M. Mito, and M. Takahashi, J. Phys. Soc. Jpn. **65**, 1934 (1996).

[12] K. R. Thurber, A. W. Hunt, T. Imai, and F. C. Chou, Phys. Rev. Lett. **87**, 247202 (2001).

[13] R. J. Baxter, *Exactly Solved Models in Statistical Mechanics* (Academic Press, London, 1982).

[14] A. A. Belavin, A. M. Polyakov, A. B. Zamolodchikov, Nucl. Phys. B **241**, 333 (1984).

[15] J. L. Cardy, *Phase Transition and Critical Phenomena*, Vol. 11, edited by C. Domb, J. L. Lebowitz (Academic Press, London, 1988).

[16] S. Eggert, I. Affleck, and M. Takahashi, Phys. Rev. Lett. **73**, 332 (1994).

[17] M. Takahashi, Prog. Theor. Phys. **46**, 401 (1971).

[18] M. Gaudin, Phys. Rev. Lett. **26**, 1301 (1971).

[19] M. Takahashi and M. Yamada, J. Phys. Soc. Jpn. **54**, 2808 (1985).

[20] P. Schlottmann, Phys. Rev. Lett. **54**, 2131(1985).

[21] M. Takahashi, in *Physics and Combinatrics*, eds. A. K. Kirillov and N. Liskova, P299-304, (World Scientific, Singapore, 2001), cond-mat/0010486.

[22] M. Shiroishi and M. Takahashi, cond-mat/0205180.

[23] M. Suzuki and M. Inoue, Prog. Theor. Phys. **78**, 787 (1987).

[24] T. Koma, Prog. Theor. Phys. **78**, 1213 (1987); *ibid* **81**, 783 (1989).

[25] A. Klümper, Z. Phys. B **91**, 507 (1993).

[26] A. Klümper, Eur. Phys. J. B **5**, 677 (1998).

[27] See for example: K. M. O'Connor and W. K. Wootters, Phys. Rev. A **63**, 052302 (2001); P. Zanardi, Phys. Rev. A **65**, 042101(2002); X. Wang, and P. Zanardi, Phys. Lett. A **301**, 1(2002).

[28] X. Wang, Phys. Rev. A **66**, 044305 (2002).

[29] S. J. Gu, H. Li,Y. Q. Li, and H. Q. Lin, Phys. Rev. A **70**, 052302 (2004).

[30] M. A. Nilesen and I. L. Chuang, *Quantum Computation and Quantum Information* (Cambridge University Press, Cambridge, England, 2000)

[31] See review article by C. H. Bennett and D. P. Divincenzo, Nature **404**, 247 (2000).

[32] A. Osterloh, Luigi Amico, G. Falci and Rosario Fazio, Nature **416**, 608 (2002).

[33] S. J. Gu, H. Q. Lin, and Y. Q. Li, Phys. Rev. A **68**, 042330 (2003).

[34] M. Takahashi, Prog. Theor. Phys. **47**, 69 (1972).

[35] M. E. J. Newman and G. T. Barkema, *Monte Carlo Method in Statistical Physics*,(Clarendon.Oxford, 1999).

[36] E. Fradkin, *Field Theories of Condensed Matter Systems*, eds. B. Holland, (Addison-Wesley Publishing Company, 1991)

[37] W. K. Wootters, Phys. Rev. Lett. **80**, 2245-2248 (1998); S. Hill and W. K. Wootters Phys. Rev. Lett. **78**, 5022-5025 (1997).